NIKA2 maps tracing dust grain evolution in cores of TMC1

C. Kramer[1], R. Adam[2], P. Ade[3], H. Ajeddig[4], S. Amarantidis[5], P. André[4], H. Aussel[4], A. Beelen[6], A. Benoît[7], S. Berta[1], M. Béthermin[8], A. Bongiovanni[5], J. Bounmy[9], O. Bourrion[9], M. Calvo[7], P. Caselli[26], A. Catalano[9], D. Chérouvrier[9], M. De Petris[10], F.-X. Désert[11], S. Doyle[3], E. F. C. Driessen[1], G. Ejlali[12], A. Ferragamo[10], A. Fuente[13], A. Gomez[13], J. Goupy[7], C. Hanser[14], S. Katsioli[15,16], F. Kéruzoré[17], B. Ladjelate[5], G. Lagache[6], S. Leclercq[1], J.-F. Lestrade[18], J. F. Macías-Pérez[9], S. C. Madden[4], A. Maury[19,20,4], F. Mayet[9], A. Monfardini[7], A. Moyer-Anin[9], M. Muñoz-Echeverría[21], I. Myserlis[5], A. Paliwal[22], L. Perotto[9], G. Pisano[10], N. Ponthieu[11], V. Revéret[4], A. J. Rigby[23], A. Ritacco[9], H. Roussel[24], F. Ruppin[25], M. Sánchez-Portal[5], S. Savorgnano[9], K. Schuster[1], A. Sievers[5], M.W.L. Smith[3], C. Tucker[3], and R. Zylka[1]

[1]Institut de RadioAstronomie Millimétrique (IRAM), Grenoble, France
[2]Université Côte d'Azur, Observatoire de la Côte d'Azur, CNRS, Laboratoire Lagrange, France
[3]School of Physics and Astronomy, Cardiff University, Queen's Buildings, The Parade, Cardiff, CF24 3AA, UK
[4]Université Paris Cité, Université Paris-Saclay, CEA, CNRS, AIM, F-91191 Gif-sur-Yvette, France
[5]IRAM, Avenida Divina Pastora 7, Local 20, E-18012, Granada, Spain
[6]Aix Marseille Univ, CNRS, CNES, LAM (Laboratoire d'Astrophysique de Marseille), Marseille, France
[7]Institut Néel, CNRS, Université Grenoble Alpes, France
[8]Université de Strasbourg, CNRS, Observatoire astronomique, UMR 7550, 67000 Strasbourg, France
[9]Univ. Grenoble Alpes, CNRS, LPSC-IN2P3, 53, av. des Martyrs, 38000 Grenoble, France
[10]Dipartimento di Fisica, Sapienza Università di Roma, Piazzale Aldo Moro 5, I-00185 Roma, Italy
[11]Univ. Grenoble Alpes, CNRS, IPAG, 38000 Grenoble, France
[12]Institute for Research in Fundamental Sciences (IPM), School of Astronomy, Tehran, Iran
[13]Centro de Astrobiología (CSIC-INTA), Torrejón de Ardoz, 28850 Madrid, Spain
[14]Aix Marseille Univ, CNRS/IN2P3, CPPM, Marseille, France
[15]National Observatory of Athens, Institute for Astronomy, Astrophysics, Space Applications and Remote Sensing, Ioannou Metaxa and Vasileos Pavlou GR-15236, Athens, Greece
[16]Department of Astrophysics, Astronomy & Mechanics, Faculty of Physics, University of Athens, Panepistimiopolis, GR-15784 Zografos, Athens, Greece
[17]High Energy Physics Division, Argonne National Laboratory, 9700 South Cass Av., Lemont, IL 60439, USA
[18]LERMA, Observatoire de Paris, PSL Research University, CNRS, Sorbonne Université, UPMC, 75014 Paris, France
[19]Institute of Space Sciences (ICE), CSIC, Campus UAB, Carrer de Can Magrans s/n, E-08193, Barcelona, Spain
[20]ICREA, Pg. Lluís Companys 23, Barcelona, Spain
[21]IRAP, CNRS, Université de Toulouse, CNES, UT3-UPS, (Toulouse), France
[22]Dipartimento di Fisica, Università di Roma, Via della Ricerca Scientifica 1, I-00133 Roma, Italy
[23]School of Physics and Astronomy, University of Leeds, Leeds LS2 9JT, UK
[24]Institut d'Astrophysique de Paris, CNRS (UMR7095), 98 bis boulevard Arago, 75014 Paris, France
[25]University of Lyon, UCB Lyon 1, CNRS/IN2P3, IP2I, 69622 Villeurbanne, France
[26]Max Planck Institute for Extraterrestrial Physics, 85748 Garching, Germany

Abstract. The Taurus Molecular Cloud TMC1 is a nearby molecular cloud filament exhibiting several dense cores. It has been intensely studied in particular because of its very rich gas phase chemistry. Here, we present NIKA2 observations with the IRAM 30m telescope of its dust emission at 1 and 2 mm wavelengths. Its vicinity of only 140 pc allows to study variations of its grain properties, i.e. its dust emissivity index β, on scales of only 2430 a.u. (18″). The NIKA2 maps are combined with Planck data to retrieve the emission at scales larger than the NIKA2 field-of-view. Maps of the 1 mm/2 mm flux ratio are then combined with a dust temperature map derived from Herschel data to create a map of the β index. Several of the observed cores exhibit a significant increase of β from $\sim$ 1.2 in the outskirts at optical extinctions of $\sim$ 5 mag to $\sim$ 1.8 in the centers at $\sim$ 18 mag. Grain models show that this steepening of the mm/submm emissivity is consistent with the gradual build-up of ice layers on the grain surfaces due to freeze-out of molecules in the cold, dense interiors of these cores.

1 Introduction

The Taurus Molecular Cloud no.1 (TMC1) is part of a network of filamentary structures which is revealed by the Herschel Gould Belt Survey (HGBS) [1]. Filaments precede the onset of most star formation, funneling interstellar gas and dust into increasingly denser concentrations that will contract and fragment leading to gravitationally bound starless cores that will eventually form stars and planets. In the cold dense interiors most molecules freeze-out [2, 3], covering the grains with icy mantles, which make them sticky, favoring grain coagulation, altering the grain size distribution, and their emissivity [4, 5]. TMC1 is a prototypical dark cloud filament at a distance of only 140 pc [6]. It is one of the closest molecular cloud complexes forming low-mass stars and has been the subject of various studies. It has been part of an IRAM 30m Large Program to study Gas phase Elemental abundances in Molecular cloudS (GEMS) [7]. The program measured the S, C, N, O depletions and ionization fraction as a function of visual extinctions in cuts through three of the TMC1 cores. Here, we discuss follow-up NIKA2 1 mm and 2 mm observations of TMC1.

2 NIKA2 observations and data processing

2.1 Camera and Observations

NIKA2 is a continuum camera at the IRAM 30m telescope allowing simultaneous observations at 1 mm and 2 mm wavelength with a field-of-view of 6.5′ using three arrays of 2900 kinetic inductance detectors (KIDs) [8–10] [1].

The NIKA2 observations cover several of the GEMS cores in Taurus and Perseus and they were conducted between 2019 and 2022 [12] in open time [2]. Here, we focus on the TMC1 region (Fig. 1). The NIKA2 observations were reduced adapting the `PIIC/GILDAS` pipeline [11][3]. The average point source flux uncertainties during all runs are 6% at 2 mm and 8% at 1 mm, resulting in uncertainties of the ratios better than 10%. The relative calibration benefits from simultaneous observations under the same conditions and in particular through the same atmosphere.

[1] NIKA2 home page: https://publicwiki.iram.es/Continuum/NIKA2/Main
[2] project IDs 105-22, 008-22, 110-21, 010-21, 096-20, 006-20, 128-19, 027-19
[3] `PIIC` home page: https://publicwiki.iram.es/PIIC

2.2 Feathering with Planck maps

To correct the NIKA2 data at both wavelengths for missing extended emission stemming from the low A_V regions surrounding the cores, we combined the NIKA2 maps with Planck maps. Here, we follow the recipe described in [13]. The Cosmic Background was not removed from the Planck maps prior to merging. Figure 2 shows how the radially averaged power spectrum at 1 mm improves the retrieval of large angular scales, i.e. scales beyond about the size of the NIKA2 field-of-view. The 2 mm power spectra behave in a very similar way. To first order, feathering of the NIKA2 with Planck data adds an offset to the NIKA2 fluxes, lowering flux ratios and β indices.

3 The dust emissivity index β at millimeter wavelengths

The observed intensities at a given frequency ν can be described by $I_\nu = \tau_\nu B_\nu(T_d) = \kappa_\nu \Sigma B_\nu(T_d)$ in the optically thin limit, with the opacity τ_ν, the Planck function B_ν, the dust temperature T_d, the emissivity cross section per gram of dust and gas κ_ν, and the gas surface density Σ. The emissivity cross section can be parametrized by $\kappa_\nu = \kappa_0(\nu/\nu_0)^\beta$ introducing the long wavelength dust emissivity slope β.

After smoothing the 1 mm map to the resolution of the 2 mm map using a Gaussian kernel, a map of the flux ratio was constructed. At the low temperatures encountered in starless cores, the Rayleigh-Jeans approximation is no longer valid. The β index is not only a function of the 1 mm/2 mm flux ratio $R_{1,2}$ but also a function of the dust temperature: $R_{1,2} = B_1(T_d)/B_2(T_d)(\nu_1/\nu_2)^{\beta_{1,2}}$. Fits of modified black-bodies to PACS and SPIRE 160, 250, 350, 500μm data from the Herschel Gould Belt Survey (HGBS) were used by [14] to create maps of dust temperature and optical extinction at 36.4″ resolution. These maps are used here to create a map of β, without further smoothing of the flux ratio map (Fig. 1). Positions with fluxes below 6σ are masked. The typical 1σ error of β is 0.13.

3.1 Map of the dust emissivity index β

In the northern and center core regions TMC1-C and TMC1-NH3 (Fig. 1) the β index increases systematically from the outskirts to the core centers, from $\sim$ 1.2 where optical extinctions are low ($A_V \sim 5$ mag) and dust temperatures are elevated ($T_\mathrm{d} \sim 16$ K) to $\sim$ 1.8 where the optical extinction is high ($A_V \sim 18$ mag) and dust temperature have dropped to $\sim$ 11 K. A part of the southern region TMC1-CP (ΔDec.$< 5'$) shows no dependence on optical extinctions with the emissivity slope staying constant at $\sim$ 1.8. The derived β values are weighted averages along the lines-of-sight which include the outer cloud envelope of more diffuse gas and dust.

3.2 Grain models

Grain models are used to interpret the β indices and their variations. Figure 3 shows dust opacity spectra modelled by [5] for proto-stellar cores. These models assume dust grains consisting of a mixture of silicates and amorphous carbon with different levels of coagulation and ice layer coverage on the agglomerates. Starting with the Mathis-Rumpl- Nordsieck (MRN) grain size distribution, a coagulation period of 10^5 years is simulated. NIR/MIR wavelengths are marked by narrow silicate and ice features while submm/mm wavelengths exhibit marked variations of the slope, i.e. of the dust emissivity index β. For bare grains, the $\beta_{1.3,0.7}$ index (i.e. the slope between 1.3 mm and 0.7 mm wavelength) drops from 1.74 to 1.23 with increasing density, when coagulation leads to increasingly large grains (Fig. 3,

Left). On the other hand, $\beta_{1.3,0.7}$ increases with increasing thickness of the ice mantles (Fig. 3, Right) from 1.5 to 1.89 for coagulated grains and a fixed density of $n_{\rm H} = 10^5$ cm^{-3}. The latter scenario is consistent with the observations in TMC1.

3.3 Discussion

A steepening of the millimeter dust emissivity slope is observed for several of the core regions in TMC1 indicating systematic changes of the dust grain properties. Here, we interpret the steepening of β as signpost of a gradual increase of the thickness of ice mantles in the inner core regions, where extinctions reach $\sim$ 20 mag, line-of-sight averaged dust temperatures are low at $\sim$ 10 K, and molecules freeze-out, consistent with the grain models of Ossenkopf & Henning (Fig. 3Right).

Previous observations of cores in nearby molecular clouds also found systematic variations of β at millimeter wavelengths. Examples are the NIKA2 study of the B10 region in Taurus [15] and the study of several other cores in Taurus and Perseus [16]. The origin of variations of the β index has been conversely discussed using different grain models. A study of several pre-stellar and protostellar cores in the B213 filament of the Taurus Molecular Cloud using NIKA [17] found significant variations of β between the cores tracing dust evolution likely due to grain-growth and dust temperature effects. In contrast, the opacity variations observed in the pre-stellar core L1544 in the Taurus molecular cloud were interpreted as stemming from uncoagulated bare grains in the outer regions and grains with thick ice mantles towards the core center [18]. A study of the star forming filament OMC 2/3 [19] attributed low values of the emissivity spectral index to millimeter sized dust grains in dense regions. However, these studies often ignore the effect of filtered large scales on the derived dust emissivities.

Future work shall derive the temperature and density profiles of the cores along the lines of sight, together with the grain properties, making use of the Abel transform. The gas-phase chemistry [7] prior to freeze-out should be linked to the dust grain chemistry.

References

[1] P. André *et al.*, Astron. Astrophys. **518**, 102 (2010)
[2] P. Caselli *al.*, Astron. Astrophys. **929**, 13 (2022)
[3] C. Kramer *et al.*, Astron. Astrophys. **342**, 257 (1999)
[4] C.W. Ormel *et al.*, Astron. Astrophys. **532**, A43 (2011)
[5] V. Ossenkopf & T. Henning, Astron. Astrophys. **291**, 943 (1994)
[6] T. Onishi *et al.*, ApJ **575**, 950 (2002)
[7] A. Fuente *et al.*, Astron. Astrophys. **624**, 105 (2019)
[8] R. Adam *et al.*, Astron. Astrophys. **609**, A115 (2018)
[9] M. Calvo *et al.*, Journal of Low Temperature Physics, **184**, 816 (2016)
[10] L. Perotto *et al.*, Astron. Astrophys. **637**, A71 (2020)
[11] S. Berta & R. Zylka, IRAM `PIIC` tutorial "Welcome to the `PIIC`" (2019-2025)
[12] C. Kramer *et al.*, EPJ Web of Conferences **293**, 27 (2024)
[13] M.W.L. Smith *et al.*, ApJS **257**, 52 (2021)
[14] J.M. Kirk *et al.*, MNRAS **532**, 4661 (2024)
[15] S. Scibelli *et al.*, MNRAS **521**, 4579 (2023)
[16] D. Navarro-Almaida *et al.*, Astron. Astrophys. **670**, A110 (2023)
[17] A. Bracco *et al.*, Astron. Astrophys. **604**, A52 (2017)

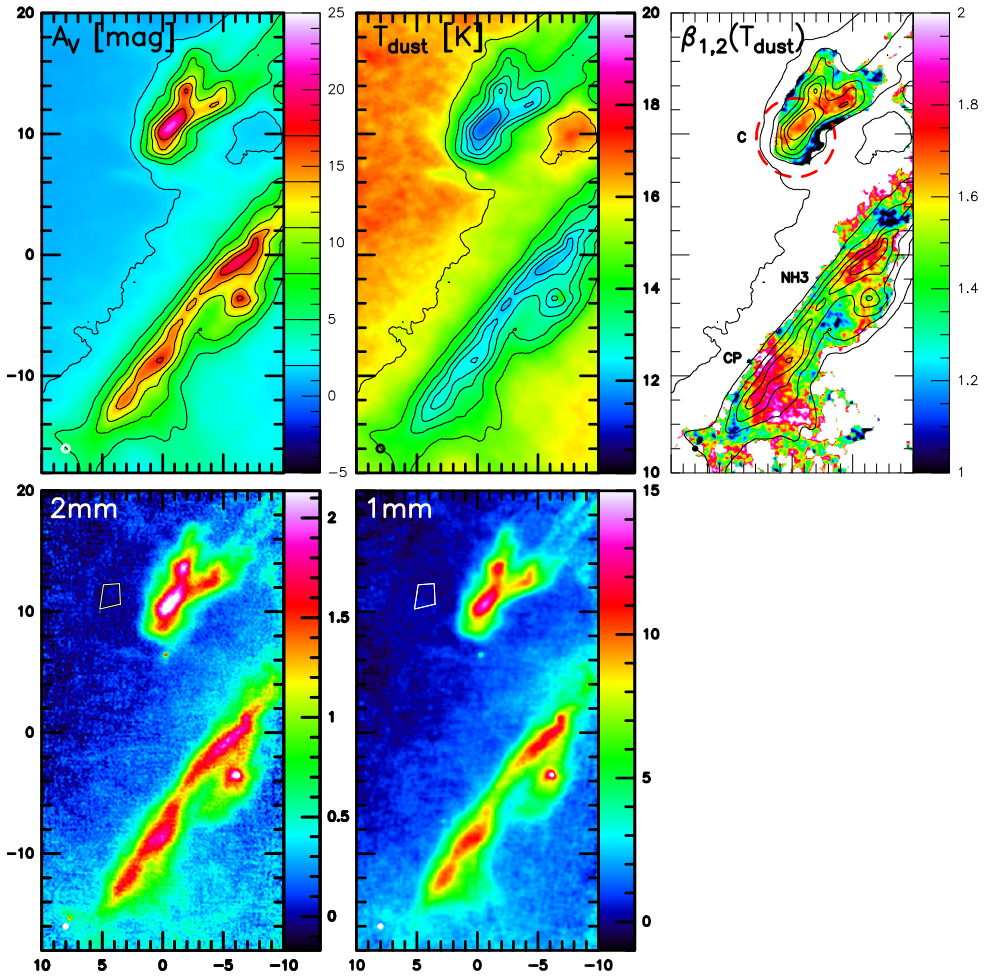

Figure 1. The TMC1 region. Lower left and right panels show NIKA2 maps combined with Planck maps at 2 mm (lower left) and 1 mm (lower right) in units of MJy/sr and at 18″ resolution. The upper left and center panels show optical extinctions and dust temperatures from Herschel HGBS data at 36″ resolution [7, 14]. The upper right panel shows the map of the dust emissivity β derived from 2 mm/1 mm flux ratios and dust temperatures. Contours show optical extinctions from 2 to 17 in steps of 3 mag. Coordinates are offsets in arcminutes. The 0/0 position is 04:41:40.0/25:50:00.0 RA/Dec (eq2000). The HPBW is given in the lower left. White polygons delineate the region selected by `PIIC` to measure the rms. The three core regions observed within the GEMS project are marked: TMC1-C, TMC1-NH3, TMC1-CP.

[18] A. Chacón-Tanarro *et al.*, Astron. Astrophys. **623**, A118 (2019)
[19] S. Schnee *et al.*, MNRAS **444**, 2303 (2014)

Ackowledgements

We would like to thank the IRAM staff for their support during the observation campaigns. The NIKA2 dilution cryostat has been designed and built at the Institut Néel. In particular, we acknowledge the crucial contribution of the Cryogenics Group, and in particular Gregory Garde, Henri Rodenas, Jean-Paul Leggeri, Philippe Camus. This work has been partially funded by the Foundation Nanoscience

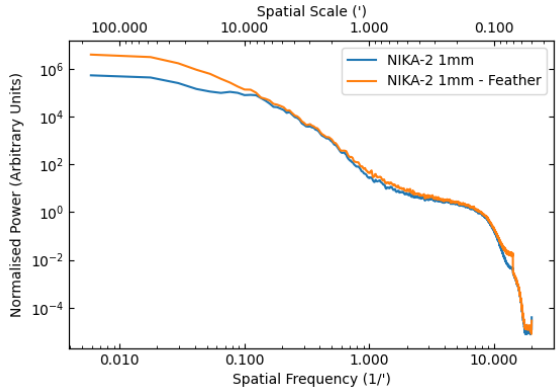

Figure 2. NIKA2 1 mm radially averaged power spectra before and after combination ("feathering") with Planck data following the recipe of [13]. The power spectra have been normalized at intermediate spatial scales. Adding the Planck data allows to retrieve the emission beyond spatial scales of $\sim 7'$ which is missed by NIKA2.

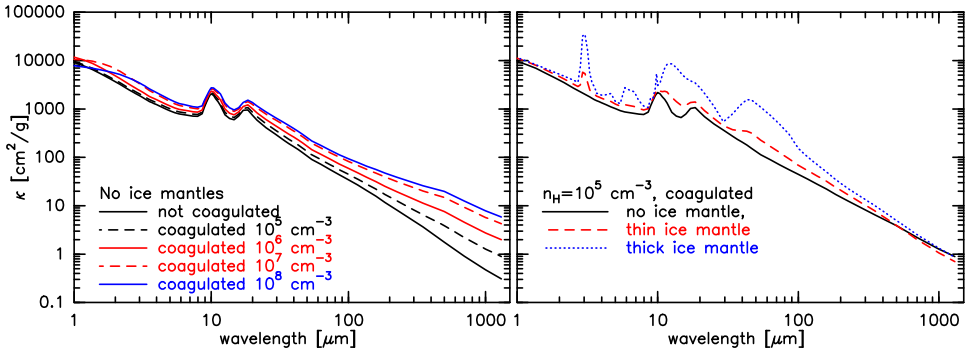

Figure 3. Modelled dust opacities [5]. **Left:** Bare grains without ice mantles, not coagulated and coagulated with increasing hydrogen densities $n_{\rm H}$. $\beta_{1.3,0.7}$ decreases from 1.74 to 1.23. **Right:** Coagulated grains with increasing ice mantle thickness at a constant hydrogen density. NIR ice features start to show-up and the dust emissivity index $\beta_{1.3,0.7}$ steepens from 1.51 to 1.89.

Grenoble and the LabEx FOCUS ANR-11-LABX-0013. This work is supported by the French National Research Agency under the contracts "MKIDS", "NIKA" and ANR-15-CE31-0017 and in the framework of the "Investissements d'avenir" program (ANR-15-IDEX-02). This work has been supported by the GIS KIDs. This work has benefited from the support of the European Research Council Advanced Grant ORISTARS under the European Union's Seventh Framework Programme (Grant agreement No. 291294). R. A. acknowledges support from the Programme National Cosmology et Galaxies (PNCG) of CNRS/INSU with INP and IN2P3, co-funded by CEA and CNES. R. A. was supported by the French government through the France 2030 investment plan managed by the National Research Agency (ANR), as part of the Initiative of Excellence of Université Côte d'Azur under reference number ANR-15-IDEX-01. A. Maury acknowledges support the funding from the European Research Council (ERC) under the European Union's Horizon 2020 research and innovation programme (Grant agreement No. 101098309 - PEBBLES). A. Fuente acknowledges funding from the European Union (ERC, SUL4LIFE, grant agreement No101096293). AF also thanks project PID2022-137980NB-I00 funded by the Spanish Ministry of Science and Innovation/State Agency of Research MCIN/AEI/10.13039/501100011033 and by "ERDF A way of making Europe".